Journal of Marine Research, 49, 281–294, 1991

Geostrophic transport of the South Equatorial Current in the Atlantic

by Lothar Stramma[1]

ABSTRACT

Geostrophic transport calculations from historical data of the equatorial South Atlantic are presented for the investigation of the flow field in the South Equatorial Current region. On the basis of water mass distribution, the potential density surface of $\sigma_1 = 32.15$ kg m^{-3} is used as a reference for geostrophic shears. This reference surface is located at a depth of 1000 to 1200 m and represents the boundary between the upper branch of the Circumpolar Deep Water and the Upper North Atlantic Deep Water. The southern band of the South Equatorial Current (SSEC) is fed by the Benguela Current, which crosses the Greenwich Meridian south of 20S. West of the Greenwich Meridian the subtropical gyre has its northernmost current band as the westward flowing SSEC. The SSEC was found to be a broad sluggish flow between 10S and 25S. The transport of the SSEC in the upper 500 m is in the order of 20 Sv, with surface velocities of around 10 cm s^{-1}. At 30W the SSEC turns northward. A small part of the water turns poleward south of 10S to form the Brazil Current, whereas the bulk of the flow contributes to the North Brazil Current and the South Equatorial Countercurrent (SECC). The SECC seems to cross the entire South Atlantic eastward to at least the Greenwich Meridian, but part of the flow might contribute to the middle branch of the South Equatorial Current flowing westward. The northernmost current band sampled is the eastward flowing South Equatorial Undercurrent. From this data no seasonality in the geostrophic field can be proven.

1. Introduction

Several multi-institutional research programs like the SEQUAL (Seasonal Equatorial Atlantic program) and the FOCAL (Programme Français Océan Climat Atlantique Equatorial) programs have been conducted in the equatorial ocean in recent years. These have resulted in substantial improvements in the description and understanding of equatorial processes, but have contributed little to the understanding of the large scale equatorial current system and its transport rates.

Classically, the Benguela Current has been portrayed as feeding into a nearly monolithic South Equatorial Current (SEC) which flows westward to the eastern promonitory of South America, Cabo de São Roque, whereupon it divides into the North Brazil Current (NBC) and the Brazil Current, with the former being stronger

1. Institut für Meereskunde, an der Universität Kiel, Düsternbrooker Weg 20, 2300 Kiel, Federal Republic of Germany.

and continuing into the northern hemisphere (Peterson and Stramma, 1991). The NBC was named 'North Brazilian Coastal Current' by Metcalf and Stalcup (1967), who first suggested that the current flowing along the northern coast of Brazil is not continuous with the Guiana Current. In recent years the name North Brazil Current has become more popular in use (e. g. Richardson and Reverdin, 1987; Carton and Katz, 1990).

A recent investigation by Reid (1989) resulted in a triangular shape of the subtropical gyre of the South Atlantic upper ocean. This is in agreement with the thermostad investigation by Tsuchiya (1986) and the inverse computations by Fu (1981) whereby it was concluded that the main westward current of the subtropical gyre should be south of 10S in the central South Atlantic and reach 10S only shortly before the Brazilian coast.

The seasonal variations of the surface currents in the tropical Atlantic were investigated by Richardson and Walsh (1986) by using ship drifts. The SEC was found to divide seasonally near the eastern tip of Brazil where residual alongshore velocities are northward for half the year (peaking during May and June) and southward for the other half of the year. Seasonal changes of dynamic topography on the sea surface relative to 500 dbar between 20S and 30N were studied by Merle and Arnault (1985). They found only a small variability in the central and western South Atlantic north of 20S. More recent results on the equatorial Atlantic annual mean ship drift, the surface geostrophic current relative to 500 dbar and the Ekman drift have been presented by Arnault (1987). Large differences exist between the surface drift found in ship drifts and surface drifters and in geostrophic surface currents. For the longitudinal average between 2S and 8S over the 12 months of the year Arnault (1987) found a westward ship drift for all longitudes and months, however, the surface geostrophic currents were eastward east of 8W except for the period between June and September when they were westward.

The geostrophic current system near the equator at 25W to 28W is quite complicated and variable. Molinari (1982) presented transport calculations for four cruises relative to 1000 m in the upper 1000 m of the tropical South Atlantic Ocean. The South Equatorial Countercurrent (SECC) was usually located between 7S and 9S. The eastward transport of the South Equatorial Undercurrent (SEUC) in the western tropical South Atlantic was estimated by Cochrane *et al.,* (1979) to have a mean value of 15 Sv (1 Sverdrup = 10^6 m^3s^{-1}) and Molinari (1982) computed a variation between 5 and 23 Sv. Surface flow above the SEUC was to the east during austral summer cruises and to the west during July and August. The SECC was observed with eastward transports ranging from 3 to 7 Sv and also showed a subsurface velocity core. Therefore, the transport of the SEC south of the equator at 25W is divided into 3 parts by the undercurrent (3–5S) and the countercurrent (7–9S). Molinari (1982) computed westward transports of 6 to 23 Sv for the northern branch (1S to the undercurrent), 7 to 26 Sv for the central branch (undercurrent to

countercurrent) and 3 Sv for the southern branch (countercurrent to 11S). With the sections only reaching from 1S to 11S, the transports of the northern and southern branch of the SEC were measured only in part. We expect that the gyre has its northern current band south of the South Equatorial Countercurrent while the southern branch of the South Equatorial Current is consequently south of 9S. In this paper we will take a closer look at the geostrophic transports in the equatorial South Atlantic.

2. The data

To describe a zonal flow mainly meridional sections are needed. Twenty five meridional sections were used: *Knorr* 2E–4W, Oct. 1983; *Discovery* 0W–4W, Apr. 1933; *Kurchatov* 2W, May 1968; *Gilliss* 2W–8W, Sep. 1973; *Geronimo* 2W–5W, Aug. 1963; *Kurchatov* 4W, May 1968; *Zvezda* 11W–12W, Sep. 1963; *Lomonosov* 15W–16W, Sep. 1963; *Explorer* 15W, Mar. 1963; *Explorer* 15.5W, Mar. 1963; *Pillsbury* 20W, Sep. 1963; *Lomonosov* 26W, Aug. 1977; A. *Saldanha* 28W, Sep. 1971; A. *Saldanha* 29W, Sep. 1971; *Hudson* 30W, Dec. 1969; *Lomonosov* 30W, Jun. 1961; *Shirshov* 30W, May 1970; *Oceanus* 30W, Feb. 1983; *Vize* 30W, Apr. 1969; *Lomonosov* 30W, May 1959; *Deutschland* 32W–34W, Aug. 1911; *Crawford* 35W, Mar./Apr. 1963; *Laserre* 34W–35W, Mar. 1963; *Laserre* 35W–36W, Sep. 1963; and *Fay* 36W–38W, Aug. 1974. Several of the meridional sections originate from the international Equalant experiment of 1963. This experiment investigated equatorial regions and these sections are restricted to the region north of about 15S.

In addition to the meridional sections one diagonal section at 30–35W by *Meteor* from Dec. 1926 and some zonal sections were used to estimate better the flow field. As zonal sections the International Geophysical Year (IGY) sections and the *Meteor* sections from 1925–1927 exist. As we had easy access to the *Meteor* data, we used the *Meteor* sections at 1–8S in Jan. 1927, at 8–12S in Sep. 1926, at 14–20S in May 1926, and at 21–23S in Jul./Aug. 1926. In addition at the southern boundary of our investigation region a section with small station spacing by *Oceanus* at 24S in Feb./Mar. 1983 was used. The diagonal section and all zonal sections are indicated by thin short dashes in Figure 1. Except for the *Meteor* data provided by the German Data Center all other data used here (Fig. 1) are from the World Oceanographic Data Center A (WODC, status 1988).

The region investigated is bounded to the east by the 1983 *Knorr* section near the Greenwich Meridian, to the west by the South American continent and to the south by two sections at 22S to 24S, which were taken by the *Oceanus* in 1983 and the *Meteor* in 1926. To the north the sections are used to a few degrees south of the equator, where the flow field becomes complicated and the normal geostrophic equations become quite sensitive to data variations and may even begin to break down. The equatorial region east of the Greenwich Meridian is not included here in the meridional sections since this region is dominated by the cyclonic gyre of the

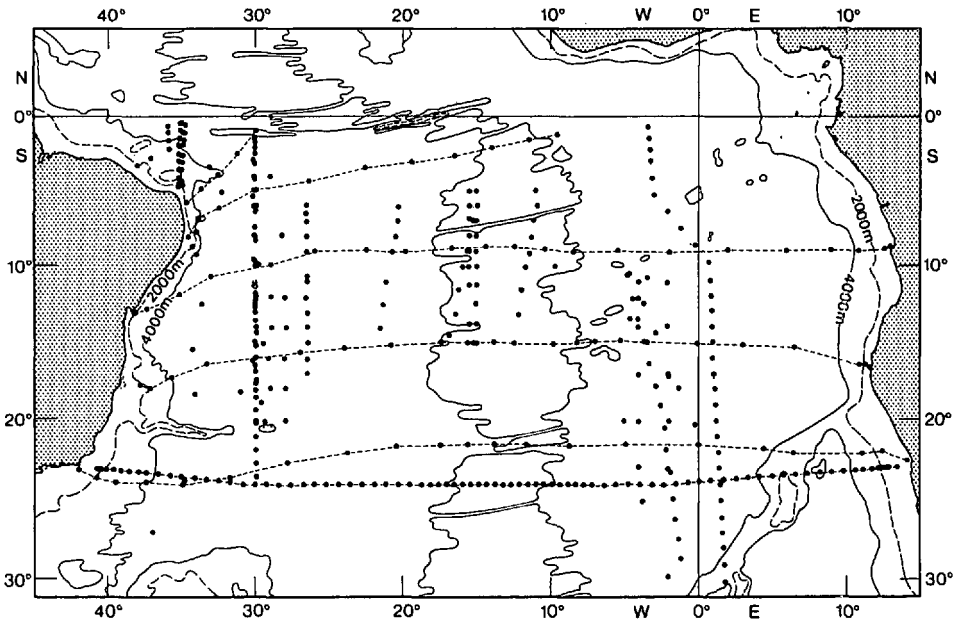

Figure 1. Positions of the hydrographic stations (dots) used here together with bottom bathymetry of 2000 m (long dashes), 4000 m (solid lines) and 6000 m (short, thick dashes). The zonal sections are indicated by thin, short dashes and the mainly meridional oriented sections are not connected.

Angola Dome (Moroshkin *et al.*, 1970; Gordon and Bosley, 1991), and because the Benguela Current, as part of the subtropical gyre south of the Angola Dome, was investigated in an earlier study (Stramma and Peterson, 1989).

First we performed a quality check on all the station data and removed the obviously incorrect values on the basis of *TS*-diagrams. Although this is a subjective procedure we believe such a hand-selected set of data is more reliable than data controlled by programs with mathematical definitions for good and bad data. One meridional section (not included in Fig. 1 and not listed before) was removed completely because of bad data quality indicated by very large scattering in the *TS*-diagrams. Some sections still show more scatter than others but the geostrophic computation results were comparable to the other sections and it is believed that the data are adequate enough to be used for the transport calculations.

3. The water masses

For geostrophic computations, a variable reference depth based on water mass properties is used. For this reason we will first take a look at the water mass distribution in the northern part of the South Atlantic. Stramma and Peterson (1989) used density layers in the Benguela Current region to define the boundaries between

water masses. For the boundary between the South Atlantic Central Water (SACW) and the Antarctic Intermediate Water (AAIW) the density σ_0 = 27.05 kg m^{-3} was used and the density σ_0 = 27.75 kg m^{-3} was used for the boundary between the upper branch of the Circumpolar Deep Water (CDW) and the Upper North Atlantic Deep Water (UNADW). In the Brazil Current region north of 20S Stramma *et al.* (1990) used the density surface σ_0 = 27.6 kg m^{-3} for the meridional sections at 30W for the boundary between CDW and UNADW. Reid (1989) showed that the CDW near the equator has a density of σ_1 = 32.1 kg m^{-3} and the upper part of the NADW has a density of σ_1 = 32.2 kg m^{-3}.

For the sections used here the parameters were plotted and the extremes transferred into the density sections. From these plots and in agreement with the values by Reid (1989), it turned out, that a density of σ_1 = 32.15 kg m^{-3} is the best choice for the boundary between CDW and UNADW. This density corresponds to σ_0 = 27.58 kg m^{-3} and therefore is close to the density of 27.6 used by Stramma *et al.* (1990) in the northwestern South Atlantic. Two examples are given in Figures 2 and 3. The figures show the distribution of the maximum and minimum in temperature, salinity and dissolved oxygen in relationship to isopycnals in the south-north sections of the equatorial region of the South Atlantic which were taken by *Explorer* in March 1963 at 15.5W (Fig. 2) and by *Crawford* in March 1963 at 35W (Fig. 3).

In the equatorial South Atlantic the upper-most water mass below the tropical surface water with a temperature of 27°C (Csanady, 1987) is the warm and salty South Atlantic Central Water, with the lower limits indicating an oxygen minimum at a depth of 300–400 m. Directly underneath is the AAIW, identified by a salinity minimum at an approximate depth of 600–800 m. On the western side of the equatorial Atlantic an oxygen maximum is located just above the salinity minimum (Fig. 3). The upper branch of the Circumpolar Deep Water is the next water mass, and is characterized by a minimum in temperature and a minimum in oxygen level on the western side near 1000 m. The deepest water mass in the upper 3000 m is the North Atlantic Deep Water. The upper branch is characterized by a weak temperature maximum and the middle branch is characterized by a salinity and oxygen maximum at a depth of 1750–2050 m.

The Figures 2 and 3 show how the density σ_1 = 32.15 kg m^{-3} is located between the extremes representing the CDW and the UNADW. The density surface σ_1 = 32.15 kg m^{-3} will be used for all the following geostrophic computations since CDW is known to flow northward while UNADW is known to flow southward.

4. Geostrophic computations

The geostrophic velocity distributions as well as the geostrophic transports were computed for all sections. Figure 4 shows the velocity distribution of the upper 1000 m in the open equatorial South Atlantic which was taken at 15W in March 1963 by the *Explorer.* South of 12S a current band of the southern branch of the SEC is

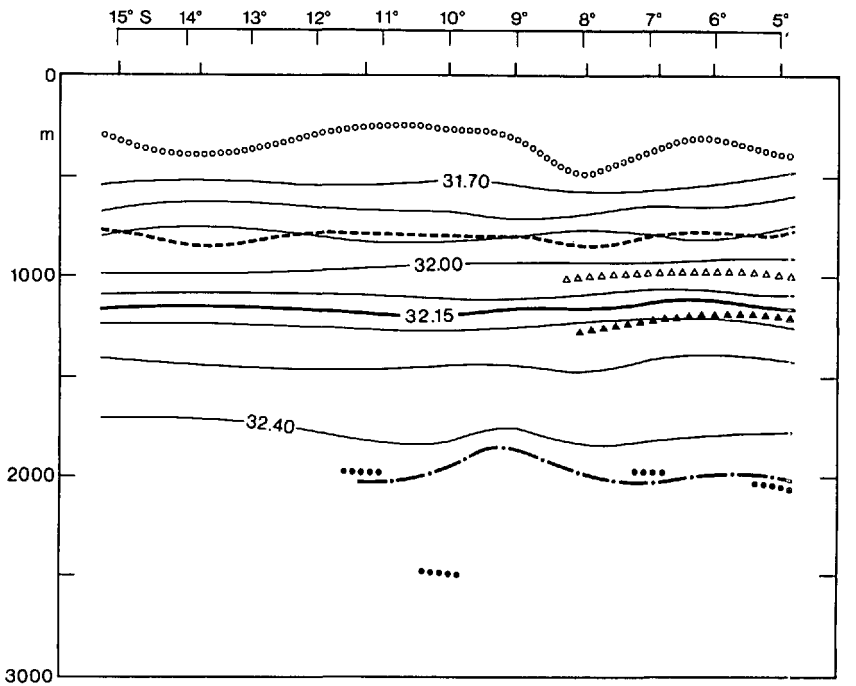

Figure 2. Vertical south-north section along 15.5W taken in March 1963 by *Explorer.* Parameter extremes are as follows: temperature maximum as solid triangles, temperature minimum as open triangles, salinity maximum as dashed-dotted line, salinity minimum as dashed line, oxygen maximum as solid circles and oxygen minimum as open circles. The σ_t isopycnals between 31.7 and 32.4 are given as lines and the σ_t = 32.15 isopycnal is included as a thick line.

visible with westward surface velocities of up to 11.3 cm s^{-1}. The highest surface velocities for the SECC were found between 9 and 10S reaching 16.4 cm s^{-1} in an eastward flow.

The section by the *Vize* in April 1969 at 30W (Fig. 5) shows the broad expansion of the southern band of the SEC at 8 to 10S and 11 to 17S. Like the surface velocities at 15W they are only approximately 10 cm s^{-1}. The SECC only reaches the sea surface at 7 to 8S, but shows an intensified subsurface velocity core at an approximate depth of 300 m. This subsurface maximum in velocity seems to be connected to the subsurface velocity core of the SEUC at 3S. The maximum eastward velocity of the SEUC with more than 20 cm s^{-1} is found at a depth of 150 m, while the surface layer above shows a westward flow. In the upper 100 m of the ocean the middle branch of the SEC shows large westward velocities near 5S.

The results of the geostrophic transport computations from the upper 500 m of the ocean for the six meridional sections along 30W are given in Table 1. The transport from the southern band of the South Equatorial Current (SSEC) is usually about

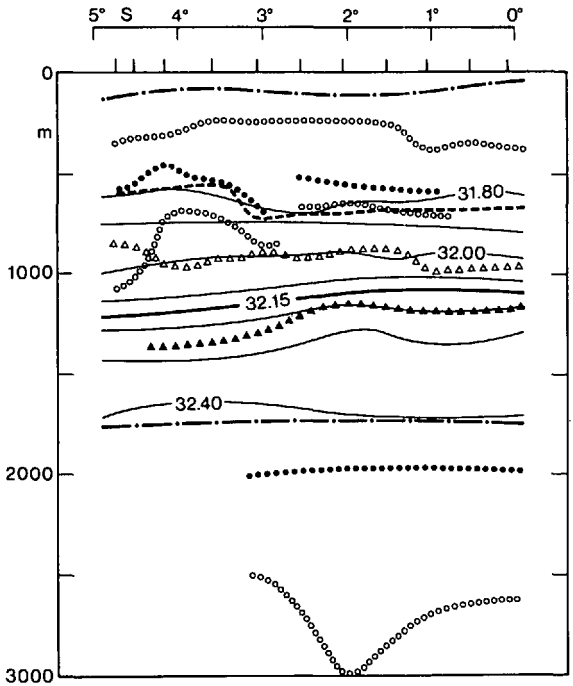

Figure 3. Vertical south-north section along 35W taken in March 1963 by *Crawford.* Parameter extremes are as follows: temperature maximum as solid triangles, temperature minimum as open triangles, salinity maximum as dashed-dotted line, salinity minimum as dashed line, oxygen maximum as solid circles and oxygen minimum as open circles. The σ_1 isopycnals between 31.8 and 32.4 are given as lines and the $\sigma_1 = 32.15$ isopycnal is included as a thick line.

20 Sv for the upper 500 m. The variability observed might be related to the different meridional extensions of the sections, possible seasonal or annual variability as well as data noise. Due to these different influences on the transport field and the uncertainty in the reference level it is not possible to present an accurate error field. Except for the section by *Shirshov* the eastward transport of the SECC was computed to be between 4.6 and 10.4 Sv in the upper 500 m which is in agreement with the 3 to 7 Sv for the SECC in the upper 1000 m at 25W to 28W (Molinari, 1982). The section by *Oceanus* with a northernmost profile at 11°50'S did not reach the region of the SECC and for this reason the transport of the SSEC is smaller than in the other sections. Just north of the eastward transport of 28.6 Sv (Table 1) in the *Shirshov* section a westward transport of 31.8 Sv can be found. Therefore, with no obvious data errors to be found in the profiles, the large eastward transport of 28.6 Sv for the SECC seems to be connected to the large westward flow just to the north.

The westward extension of the current bands can be investigated with the section by *Crawford* in April 1963 at 35W (Figure 6), just north of the Brazilian coast. The

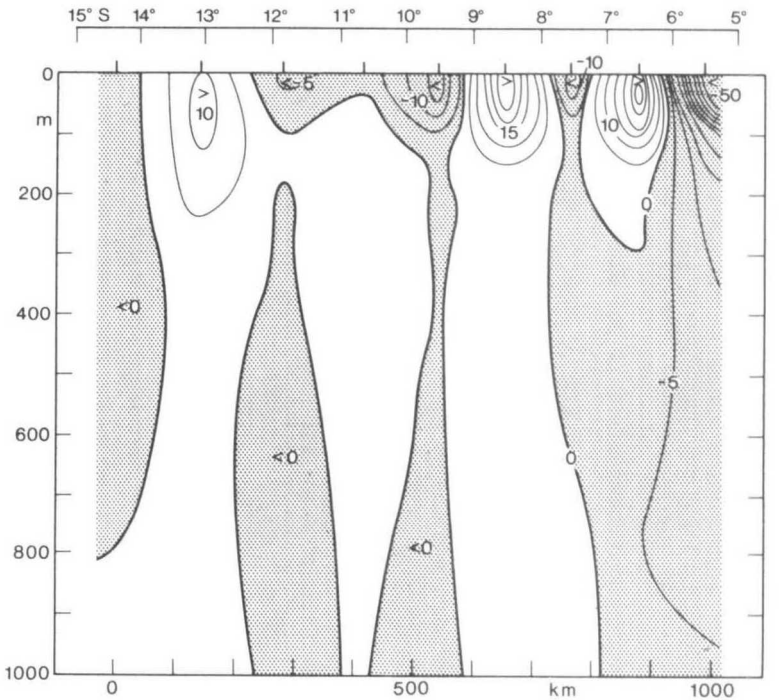

Figure 4. Geostrophic velocity distribution with an isoline spacing of 5 cm s^{-1} relative to the isopycnal $\sigma_1 = 32.15$ kg m^{-3} from the *Explorer* section at 15W in March 1963. Positive velocity is westward, negative velocity is directed eastward and indicated by shaded areas. Short tick-marks on the top show the mid-points between stations.

water of the South Equatorial Current splits into the southward flowing Brazil Current and the North Brazil Current at about 10S off the coast (Stramma *et al.*, 1990). The NBC at 35W is found to be an intense current band near the coast with velocities of up to 90 cm s^{-1} at 4S. At 3S the SEUC is found as a subsurface current between 100 m and 1000 m while the surface flow is directed westward again. A band of the westward flowing SEC is located between 2 and 3S.

A schematic representation of the geostrophic flow field based on our data has been constructed to fit the transport results of the sections and is shown in Figure 7. All meridional and zonal sections listed in chapter 2 were used. The geostrophic transports between all station pairs were written into the station net of Figure 1 and the resulting transport lines were drawn. This is a subjective procedure but a mathematical interpolation scheme would be influenced by eddy-like features with large transports in opposite directions which were ignored in the hand contoured flow field. Because of mass imbalances resulting from the non-synoptic sections this field does not closely fit all the transport estimates of all sections. However, this field shows the essential qualities of the flow. As described already by Stramma and Peterson (1989) the Benguela Current leaves the African coast farther south and

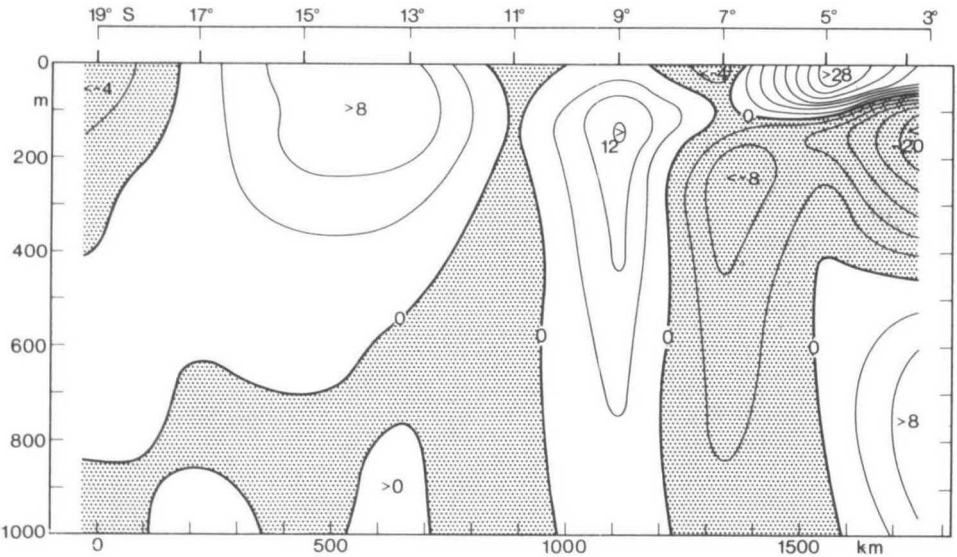

Figure 5. Geostrophic velocity distribution with an isoline spacing of 4 cm s^{-1} relative to the isopycnal σ_1 = 32.15 kg m^{-3} from the *Vize* section at 30W in April 1969. Positive velocity is westward, negative velocity is directed eastward and indicated by shaded areas. Short tick-marks on the top show the mid-points between stations.

most of the upper ocean transport crosses the Greenwich Meridian south of 20S. West of the Greenwich Meridian the water of the subtropical gyre flows westward as a broad and sluggish flow between 10S and 25S, and is called the South Equatorial Current. Since the westward flows in the South Atlantic north of 10S are also called SEC (e.g. Katz, 1981), the northern component of the subtropical gyre with its flow south of 10S is, therefore, the southern band of the SEC (SSEC).

At or west of 30W the SSEC turns northward (Fig. 7). A part of the water of the SSEC turns south to form the Brazil Current when reaching the Brazilian coast south of 10S (Stramma *et al.*, 1990), while the larger amount of water flows either to the north and then to the northwest to contribute to the North Brazil Current or turns east to form the SECC. The SECC seems to cross the entire South Atlantic at about 7 to 9S to at least the Greenwich Meridian but part of the water might get lost and contribute to the central branch of the SEC flowing westward at about 5S. Figure 7 shows the eastward flowing SEUC at about 3S as the northernmost current band which is only partly determined by our data. The existence of the SEUC and the SECC at 5W can already be seen in the velocity distributions of January and July 1975 as shown by Hisard *et al.* (1976). With the data used here our Figure 7 shows that the water contributing to the Brazil Current comes from farther south when compared to the flow field in the northern Brazil Current region derived by Stramma *et al.* (1990). This large inflow from the south is mainly the result of the use of two

Table 1. Geostrophic transports (*Tr*) at 30W from the surface to a depth of 500 m depth in Sv (positive westward) relative to a given density reference σ_1 (Sig) for the SECC at about 8S and the southern band of the SEC (SSEC). The SSEC transport is for the entire section south of the SECC while SECC represents the eastward flow of the section at about 8S, if available.

Ship	Longitude	Time	Reference Sig	Reference depth (m)	Section used from to	SSEC *Tr*	SECC *Tr*
Oceanus	30W	Feb. 1983	32.15	1100-1150	11°50′-23°32′S	14.6	—
Vize	30W	Apr. 1969	32.15	1060-1090	5°59′-20° 0′S	21.9	−8.4
Lomonosov	30W	May 1959	32.15	1100-1180	6° 1′-20° 2′S	17.9	−4.9
Shirshov	30W	May 1970	32.15	1070-1360	6°22′-20° 3′S	25.8	(−28.6)
Lomonosov	30W	Jun. 1961	32.15	980-1180	6° 2′-20° 1′S	32.1	−10.4
Hudson	30W	Dec. 1969	32.15	1110-1140	7°27′-20° 0′S	18.6	−4.6

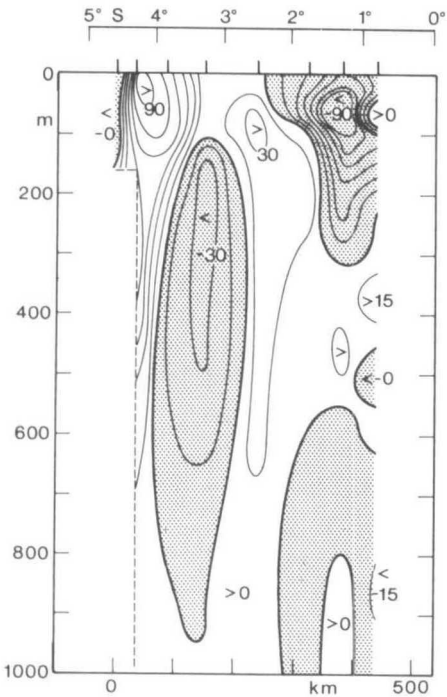

Figure 6. Geostrophic velocity distribution with an isoline spacing of 15 cm s^{-1} relative to the isopycnal $\sigma_t = 32.15$ kg m^{-3} from the *Crawford* section at 35W in April 1963. Positive velocity is westward, negative velocity is directed eastward and indicated by shaded areas. Short tick-marks on the top show the mid-points between stations.

southernmost zonal sections at about 23S which contribute more water flowing north than was found in the data near 20S used by Stramma *et al.* (1990).

We investigated whether seasonality can be found by dividing the data set into the periods of December to May and June to November. With this reduced data set it was not possible to prove a seasonal signal in the large scale flow since the changes observed were in the same order as the variability between the different sections. This weak variability is in agreement with the findings of Merle and Arnault (1985), who found only small variability in the central and western South Atlantic in dynamic topography. Results by Molinari (1983) imply that the geostrophic component of the SEC is strongest during the austral winter and that an eastward surface flow may divide a weaker SEC into two branches at about 25W north of 10S during austral summer. Based on Richardson and McKee's (1984) ship drift maps Csanady (1985) gave transport estimates of 30 Sv for the SEC as a source of the NBC in the months of July to December and of 10 Sv for January to July. A different signal can be extracted from the maps of Cochrane *et al.* (1979). It seems as if the North Brazil Current is weaker in July-September and stronger in February-April. The sections used here at 35W didn't prove a seasonal signal for the NBC: In April 1963 the *Crawford* data of

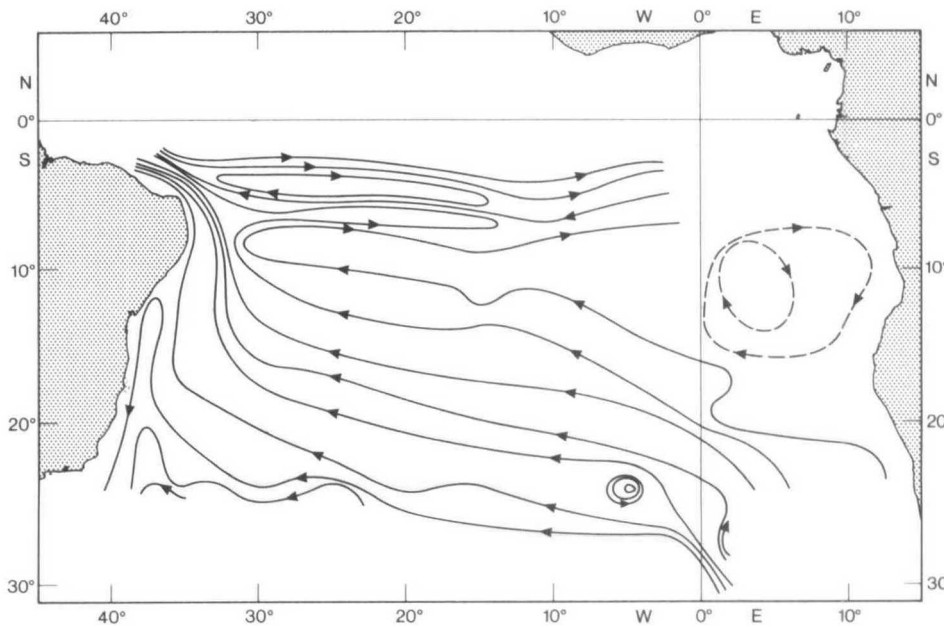

Figure 7. Schematic representation of the geostrophic flow field in the upper 500 m based on all the stations from Figure 1. The solid flow lines represent a transport of 3 Sv. The broken flow line represents the Angola gyre from our small set of data on this region with the shape according to Gordon and Bosley (1991).

the upper 500 m for the NBC resulted in a transport of 18.9 Sv and in March 1963 the *Laserre* data showed 14.6 Sv for the NBC and in August/September 1962 the transport of the *Laserre* section showed a NBC of 14.3 Sv between 35W and 33W. With regard to data noise and interannual changes the differences are within a possible variability range.

5. Discussion

In this study we used the available historical data to map the general geostrophic flow field of the surface layer of the northern part of the South Atlantic Ocean and to compute the geostrophic transports and velocities of the SSEC on meridional sections. Although some of our data are not of the highest quality, the pattern we have obtained should be fairly accurate.

As indicated in earlier investigations (e.g. Fu, 1981; Reid, 1989) the SSEC, as the northern band of the subtropical gyre of the South Atlantic, crosses the ocean south of 10S. The shape of the flow field of the SSEC derived here is in agreement with these earlier investigations. Compared to these former papers the geostrophic velocity distribution and the transports along meridional sections at different locations were computed. The zonal transport shown by Fu (1981) are only the residual of some zonal sections about 8° latitude apart while Reid (1989) presented as

transport field only the top to bottom flow of the entire South Atlantic. Meridional sections had been used before by Molinari (1982), but only north of 11S. Therefore, transport estimates on meridional sections for a comparison with our results are missing.

With the South Atlantic Current at about 40S (Stramma and Peterson, 1990) and the Benguela Current leaving the African coast farther south, the subtropical gyre of the South Atlantic becomes more triangular in shape than the gyre in the North Atlantic. Only at and west of 30W does the upper ocean transport of the SSEC turn north and contribute water to the Brazil Current, the North Brazil Current and the SECC. The SSEC is found to be a broad and sluggish flow between 10S and 25S. Only near the Brazilian coast do the currents appear more condensed with increased flow velocities.

As pointed out by Peterson and Stramma (1991), the zero-line of the annual mean curl of wind stress in the lower latitudes of the South Atlantic is oriented diagonally across the basin from near Cape Town to equatorial latitudes north of the northern coast of Brazil (see their Fig. 6). This line is located just to the north of where the SSEC is found. Stramma *et al.* (1990) discussed the influence of the annual mean curl of the wind stress on the loss of water from the subtropical gyre to the North Brazil Current, which could be a mechanism leading to the overall weakness of the Brazil Current. The loss of water by the NBC could easily be compensated for by the flux in the Ekman layer, which Roemmich (1983) estimated in the annual mean in the South Atlantic as being 13.7 Sv in the South Atlantic southward across 8S.

It is surprising that very little is known about the southern band of the South Equatorial Current, although a systematic investigation including transport estimates (Wüst, 1957) for the South Atlantic was completed with the *Meteor* expedition from 1925 to 1927. The lack of data on the meridional sections crossing the SSEC is a problem and also proved to be a problem in this study. As seen in Figure 1 all meridional sections in the central South Atlantic contain only data north of about 15S. Therefore, the flow field south of 15S and north of the zonal sections at about 23S had to be interpolated, which led to inaccuracies in the location of the schematic flow field. Consequently, meridional sections from the equator to about 30S are needed to investigate the SEC in more detail. In fact, some sections have been made in the past few years, but the data are not yet available to us.

Acknowledgments. This work was supported in part by the Bundesminister für Forschung und Technologie grant MFG0086-0 and by the Deutsche Forschungsgemeinschaft grant SFB-133 both in Bonn, Federal Republic of Germany.

REFERENCES

Arnault, S. 1987. Tropical Atlantic geostrophic currents and ship drifts. J. Geophys. Res., *92,* 5076–5088.

Carton, J. A. and E. J. Katz. 1990. Estimates of the zonal slope and seasonal transport of the Atlantic North Equatorial Countercurrent. J. Geophys. Res., *95,* 3091–3100.

Cochrane, J. D., F. J. Kelly Jr. and C. R. Olling. 1979. Subthermocline countercurrents in the western equatorial Atlantic Ocean. J. Phys. Oceanogr., *9,* 724–738.

Csanady, G. T. 1985. A zero potential vorticity model of the North Brazilian Coastal Current. J. Mar. Res., *43,* 553–579.

—— 1987. What controls the rate of equatorial warm water mass formation? J. Mar. Res., *45,* 513–532.

Fu, L.-L. 1981. The general circulation and meridional heat transport of the subtropical South Atlantic determined by inverse methods. J. Phys. Oceanogr., *11,* 1171–1193.

Gordon, A. L. and K. T. Bosley. 1991. Cyclonic gyre in the tropical South Atlantic. Deep-Sea Res., (in press).

Hisard, P., J. Citeau and A. Morlière. 1976. Le système des contre-courants équatoriaux subsuperficiels, permanence et extension de la branche sud dans l'océan atlantique. Cah. O.R.S.T.O.M., sér. océanogr., *14,* 209–220.

Katz, E. J. 1981. Dynamic topography of the sea surface in the Equatorial Atlantic. J. Mar. Res., *39,* 53–63.

Merle, J. and S. Arnault. 1985. Seasonal variability of the surface dynamic topography in the tropical Atlantic Ocean. J. Mar. Res., *43,* 267–288.

Metcalf, W. G. and M. C. Stalcup. 1967. Origin of the Atlantic Equatorial Undercurrent. J. Geophys. Res., *72,* 4959–4975.

Molinari, R. L. 1982. Observations of eastward currents in the tropical South Atlantic Ocean: 1978–1980. J. Geophys. Res., *87,* 9707–9714.

—— 1983. Sea-surface temperature and dynamic height distributions in the central tropical South Atlantic Ocean. Oceanologica Acta, *6,* 29–34.

Moroshkin, K. V., V. A. Bubnov and R. P. Bulatov. 1970. Water circulation in the eastern South Atlantic Ocean. Oceanology, *10,* 27–34.

Peterson, R. G. and L. Stramma. 1991. Upper-level circulation in the South Atlantic Ocean. Prog. in Oceanogr., *26,* 1–73.

Reid, J. L. 1989. On the total geostrophic circulation of the South Atlantic Ocean: Flow pattern, tracers, and transports. Prog. in Oceanogr., *23,* 149–244.

Richardson, P. L. and T. M. McKee. 1984. Average seasonal variations of the Atlantic North Equatorial Countercurrent from ship drift data. J. Phys. Oceanogr., *14,* 1226–1238.

Richardson, P. L. and G. Reverdin. 1987. Seasonal cycle of velocity in the Atlantic North Equatorial Countercurrent as measured by surface drifters, current meters, and ship drifts. J. Geophys. Res., *92,* 3691–3708.

Richardson, P. L. and D. Walsh. 1986. Mapping climatological seasonal variations of surface currents in the tropical Atlantic using ship drifts. J. Geophys. Res., *91,* 10537–10550.

Roemmich, D. 1983. The balance of geostrophic and Ekman transports in the tropical Atlantic Ocean. J. Phys. Oceanogr., *13,* 1534–1539.

Stramma, L., Y. Ikeda and R. G. Peterson. 1990. Geostrophic transport in the Brazil Current region north of 20S. Deep-Sea Res., *37,* 1875–1886.

Stramma, L. and R. G. Peterson. 1989. Geostrophic transport in the Benguela Current region. J. Phys. Oceanogr., *19,* 1440–1448.

—— 1990. The South Atlantic Current. J. Phys. Oceanogr., *20,* 846–859.

Tsuchiya, M. 1986. Thermostads and circulation in the upper layer of the Atlantic Ocean. Prog. in Oceanogr., *16,* 235–267.

Wüst, G. 1957. Stromgeschwindigkeiten und Strommengen in den Tiefen des Atlantischen Ozeans. Wiss. Erg. der dt. Atlant. Exped. Meteor 1925–1927, 6, Teil 2, 6. Lieferung, 261–420.

Received: *6 September, 1990;* revised: *28 February, 1991.*